RFQ VANE SHAPES FOR EFFICIENT ACCELERATION

Y. Iwashita, Y. Fuwa, ICR, Kyoto Univ. Uji, Kyoto
R. A. Jameson, IAP, Frankfurt am Main

Abstract

RFQ vane shapes for efficient acceleration are under investigation by introducing more terms in addition to the two-term potential. They can incorporate the feature of the trapezoidal shape modulation with less multipole components, while higher acceleration efficiency is expected. A series of electrostatic calculations was carried out for a new 7-term potential ones. They are compared with the two-term scheme and the trapezoidal scheme. The new one exhibits a higher accelerating efficiency with less multipole components.

INTRODUCTION

Design of RFQ has been based on the so-called two-term potential scheme [1]. The two-term potential has the minimum terms of acceleration and focusing in the lowest order:

$$U_2(r,\theta,z)=\frac{V}{2}\left\{X\left(\frac{r}{a}\right)^2\cos 2\theta + AI_0(kr)\cos(kz)\right\}$$

where

$$A=\frac{m^2-1}{m^2I_0(ka)+I_0(mka)},\quad k=\pi/Lc$$

and a is the minimum radius at z=0 (see Fig. 1)[2]. The vane surface profile can be defined by the equipotential surface of U_2 at the vane voltage $V/2$. These parameters are independently defined at each cell, which may make discontinuities between cells if no care is taken for it.

The acceleration term A and the focusing term X are the functions of only m and Lc/a. A contour plots of A as function of m and Lc/a is shown in Fig.2. Since the acceleration term A does not increase monotonicaly with m in the short cell length region when the minimum aperture a is kept constant, m is usually limited up to 2 or 3 for practical cases. This can be comprehended by observing the vane surface profiles in such regions, where the ridgeline of the equipotential surface breaks [3]. The practical m values is a function of Lc/a, which can be roughly expressed by m < 1.3+0.6(Lc/a-0.75) and is expressed by a red line in Fig. 2.

While the set of Lc/a and m is simple to define the potential, the set of Lc/r_0 and m is often used. In this case, the potential is rewritten as follows:

$$U_2(r,\theta,z)=\frac{V}{2}\left\{\left(\frac{r}{r_0}\right)^2\cos 2\theta + AI_0(kr)\cos(kz)\right\}$$

where

$$r_0=a/\sqrt{1-AI_0(ka)},\ A=\frac{m^2-1}{m^2I_0(ka)+I_0(mka)},\quad k=\pi/Lc$$

Figure. 3 shows the same contour plot but as a function of Lc/r_0 and m. The large m at short Lc region not for use is expresed by the red curve in Fig. 3.

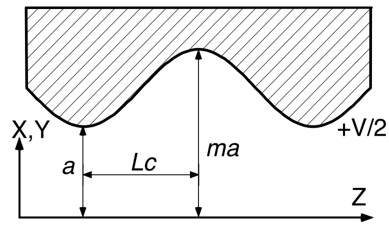

Figure 1: Definitions of vane parameters.

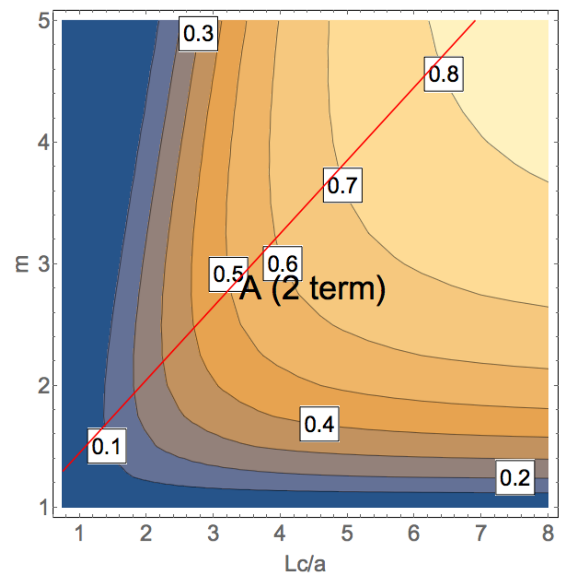

Figure 2: Contour plot of the acceleration term A as a function of Lc/a and m for the two-term potential.

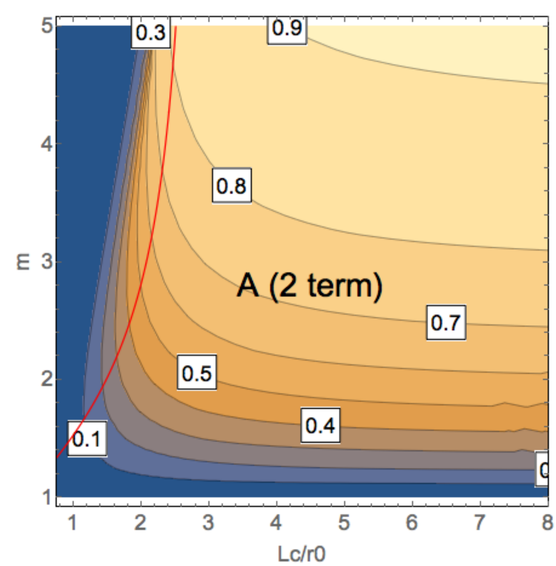

Figure 3: Contour plot of the acceleration term A as a function of Lc/r_0 and m for the two-term potential.

ISBN 978-3-95450-169-4

SEVEN-TERM POTENTIAL

Trapezoidal vane shapes can exhibit the higher acceleration efficiency. The shapes, however, generate higher multipole terms in the beam bore region. Thus, it should be desirable if vane shapes with higher accelerating efficiency and less multipole component can be synthesized from only the two parameters Lc/r_0 and m without too much complexity for data to NC machines. One possibility is to use the following expression:

$$U_7(r,\psi,z)=\frac{V}{2}\{\cos 2\psi\,(a_{01}\left(\frac{r}{a}\right)^2+a_{11}I_2(kr)\cos(kz)+$$
$$a_{21}I_2(2kr)\cos(2kz))+\sum_{i=1,3,5,7}a_{i0}I_0(ikr)\cos(ikz)\}$$

a_{01}: Constant Q term for conventional RFQ,
a_{11}: Inter Cell Continuity (New),
a_{21}: IH DTL type Q (finger) & Trapezoid,
a_{10}: Basic accelerating Term,
a_{30}~a_{70}: Other accelerating terms (New).
The parameters can be define by setting the conditions:

$$U_7(a,0,0)=U_7(ma,0,Lc)=V/2,$$
$$\left.\frac{d^2}{dz^2}U_7(a,0,z)\right|_{z=0}=\left.\frac{d^2}{dz^2}U_7(ma,0,z)\right|_{z=Lc}=0,$$
$$\left.\frac{d^3}{dz^3}U_7(ma,0,z)\right|_{z=Lc}=\left.\frac{d^4}{dz^4}U_7(ma,0,z)\right|_{z=Lc}=0$$

The first two conditions set the radial positions of the ridge at both the edges and the other four conditions make the ridge flatter at both the edges (see Fig.4). The a_{11} papameter is determined to keep the C0 continuity of the ridgeline between adjacent cells. They should be uniquely detemined by applying the continuity condition from the upstream cells. These seven conditions can be solved to define the a_{xx} parameters and U_7 can also be a function of Lc/a and m. This enables the design procedure similar to the current one.

The effective acceleration factor AT including the transit time factor T is important index for discussions of acceleration efficiency. In order to compare the acceleration efficiency, AT factor of the 7-term potentials is shown in Fig. 5. The ratio between the two cases is shown in Fig 6. As can be seen, the AT term is up to 15% higher in 7-term case.

A typical vane surface generated from such a multi-term potential is shown in Fig. 7. Because the higher order terms inflate as the radial coordinate becomes larger, the fringes become very wavy, which should be eliminated for practical reasons. By checking the transverse crosssection shape of vanes, the shape does not change much along the axis and at the z=0 position where the aperture is minumum is always close to a hyperbola curve. This is consistent with the fact that the main mulpole component is a quadrupole. Since the prominent surface that is close to the axis is the most dominant part, some shape discrepancy at other location may be ignored. Thus we may use constant transverse crosssection of a part of a hyperbola along the cell axis. Because the hyperbola shape is defined by a, the ridge continuity is guaranteed at $r=a$. The possible step at $r=ma$ can be removed by the a_{11} term if necessary, while only the ridge line can be C0 continuous with this method. An area

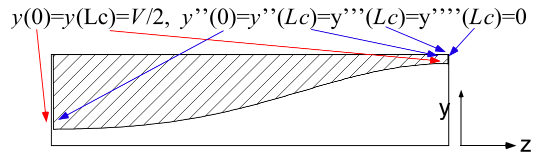

Figure 4: Conditions for vane parameters.

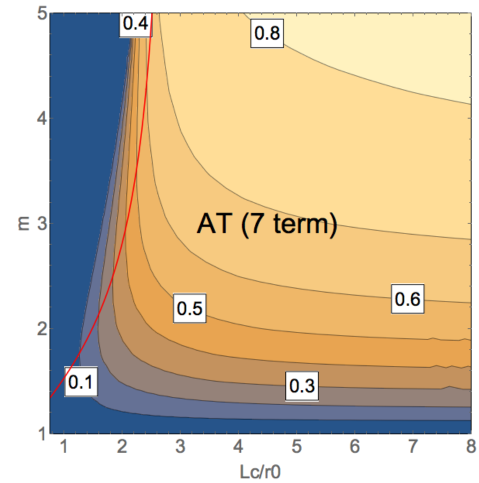

Figure 5: Contour plot of the acceleration term AT as a function of Lc/r_0 and m for the seven-term potential.

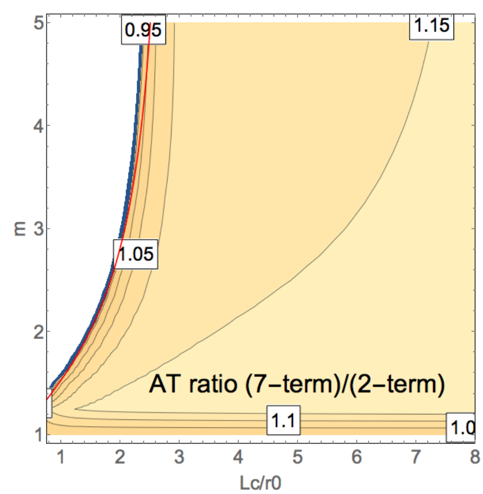

Figure 6: Ratio of acceleration term AT of 7-term to that of 2-term as a function of Lc/r_0 and m.

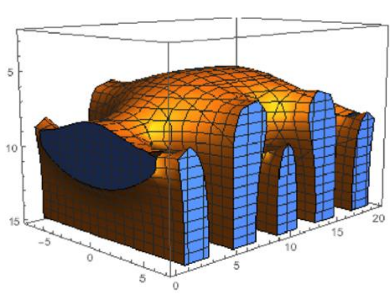

Figure 7: A typical vane shape generated from multi-term potential. The Higher order terms make the fringes wavy, which should be eliminated. (Lc/a=2, m=1.5)

far from the axis is not dominant to the electric field distribution in the beam axis and the continuity should be less important. Figure 8 shows a typical vane profile that uses the constant hypaebolic crosssection at r=a along the beam axis. The ridge shape is close to that of trapezoidal shape.

3D-CALCULATIONS

Because the vane shapes are approximated for elimination of the wavy fringes, 3D-calculations were performed for the vane shapes generated from the proposed method. Figure 9 shows a typical geometry of the electrode, where only the horizontal vane is shown.

Three geometries are compared: 1) constant sinusoidal modulation, 2) 40% slope trapezoidal modulation and 3) the 7-term potential case. The cross-section of the first two is a constant circular one with the radius R =0.75rr, where rr=a(m+1)/2 and 10° straight skirt lines. The first one is approximation of the 2-term one. The 7-term one has 0° straight skirt lines. The calculated AT factors for the three cases are shown in Fig. 10. AT factor is larger than the sinusoidal one and close to the trapezoidal one. The a_{03} term is smaller than the other two cases at the small m region. The behaviour at other region may be improved by a modification of the cross-section shape.

SUMMARY

New series of the vane shapes are proposed. The vane shape is a function of m and Lc/a or Lc/r_0 like one generated from the 2-term potential. They exhibit larger accelerating factor than two-term potential. The wavy fringe can be eliminated using a constant cross section defined at the vane top.

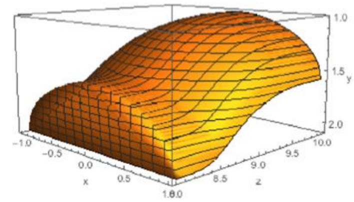

Figure 8: A typical geometry of the electrode for 3-D calculation.

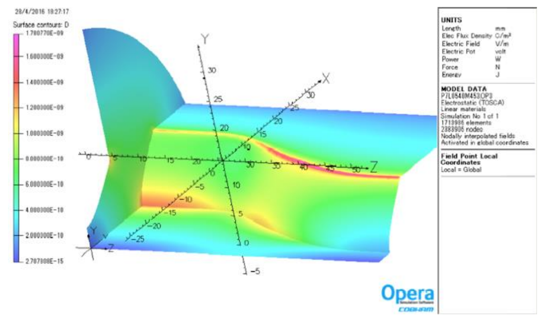

Figure 9: A typical vane shape generated from the proposed method using a constant hyperbolic cross-section. The fringe area is rounded in this example.

REFERENCES

[1] R. H. Stokes, K. R. Crandall, J. E. Stovall and D. A. Swenson, RF QUADRUPOLE BEAM DYNAMICS, IEEE Trans. Nucl. Sci. NS-26, 3, 1979, pp.3469-3471

[2] K. R. Crandall, Effects of Vane-Tip Geometry on the Electric Fields in Radio-Frequency Quadrupole Linacs, LA-9695-MS

[3] Y. Iwashita, Y. Fuwa, New Series of RFQ Vane Shapes, Proc. IPAC2015, Richmond, pp.3808-3810

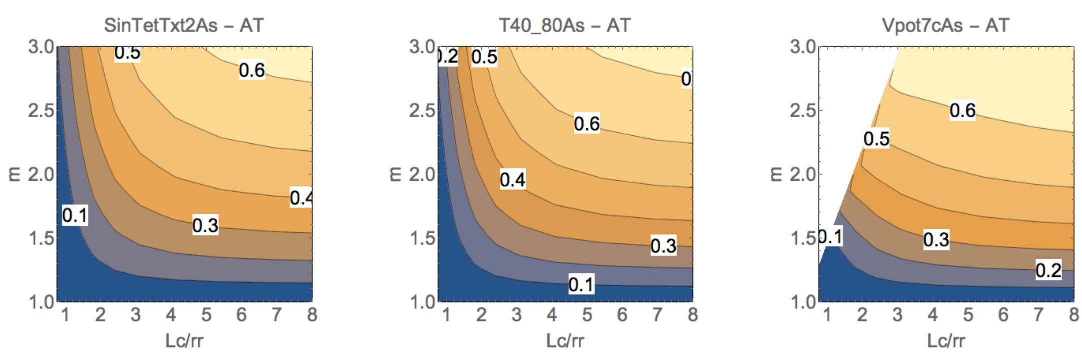

Figure 10: Results of 3-D calculation for AT.

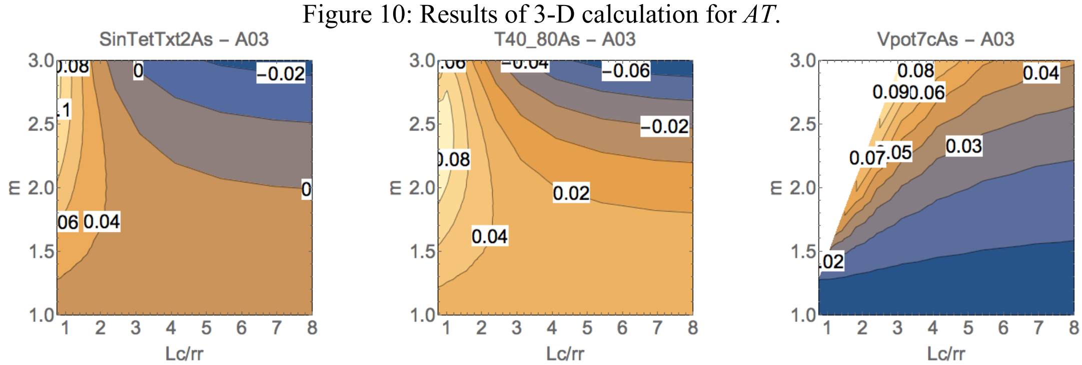

Figure 11: Results of 3-D calculation for A03 (dodecapole).

ISBN 978-3-95450-169-4